Environ. Sci. Technol. **1996**, *30,* 3243−3249

Numerical and Experimental Study of Cleaning Process of a Pulse−Jet Fabric Filtration System

HSIN-CHUNG LU AND CHUEN-JINN TSAI*

Institute of Environmental Engineering, National Chiao-Tung University, No. 75 Poai Street, Hsinchu, Taiwan

A numerical model was developed to simulate the unsteady, compressible pulse−jet cleaning process for a fabric filtration system. The objective is to find the best design and operating conditions that provide more cleaning force for bag cleaning. The simulated results of air pressure and flow distributions in the system agree reasonably well with the experimental data. The study shows that tank volume, initial tank pressure, nozzle diameter, distance between nozzle and bag top, and pulse duration are the major parameters influencing the pressure impulse in the fabric bag. For the system investigated, the optimized nozzle diameter is 30 mm, pulse duration is from 300 to 600 ms, distance between nozzle and bag top is 60 cm, and tank volume is 0.3−0.5 m^3. Given all other conditions fixed, increasing the tank pressure seems to be the most convenient way to achieve a higher bag cleaning efficiency. A new bag was used in this study that has a resistance coefficient of 864 Pa·s m^{-1}. The study shows that the major effect of increasing the resistance coefficient to as much as 10 times that of a clean bag is to increase the pressure pulse in the bag. The optimum design parameters remain unchanged.

Introduction

The pulse−jet fabric filter system is the emerging main stream among various fabric filter designs. In a pulse−jet fabric filtration system, dust particles are collected outside of the fabric bags. When the pressure drop across the system is greater than a designated value (e.g., 4 in. of H_2O), a short burst of air is fired into the open end of cylindrical bags through a pulse valve. The sudden increase of air pressure inside the bags leads to an acceleration of the filter cloth, resulting in the removal of the dust cake. Typical components of a pulse−jet cleaning system include air pressure tank, pulse valve, blow tube, nozzle, fabric bag, and/or venturi.

Because of its higher cleaning efficiency, the pulse−jet fabric filter is able to use a higher filtration velocity than other fabric filtration systems. Many design and operational parameters can influence the performances of pulse−jet fabric filters, including tank volume, tank pressure, blow tube diameter, pulse valve discharge characteristics, nozzle diameter, pulse duration, dust and fluid properties, etc.

Bustard et al. (*1*) selected three of the common pulse−cleaning designs representing low pressure (LP), intermediate pressure (IP), and high pressure (HP) cleaning methodologies to evaluate pulse−jet fabric filter performance for U.S. fossil-fuel-fired applications. In the LP configuration, the tank pressure reaches approximately 12 psi, and no venturi is used at the bag top. In the HP configuration, a venturi is installed at the bag top to induce secondary flow and to direct the air flow along the length of the bag. They concluded that the LP, IP, and HP pulse−cleaning systems are all able to maintain the baghouse pressure drop between 4 and 6 in. of H_2O, although the HP and IP systems require a higher cleaning frequency than the LP system. The EPRI report (*2*) compared the performances of the "advanced" and traditional high-ratio fabric filter designs. The former system utilizes 15−30 psi compressed air to pulse into bag and no venturi is used at the bag, the latter system utilizes 70−90 psi compressed air and a venturi is installed at the bag top. EPRI found that for an equivalent cleaning efficiency, the advanced design requires lower tank pressure, longer bag length, and lower cleaning energy.

Many different bag cleaning parameters such as peak pressure, initial pressure rise rate, fabric acceleration, and pressure impulse in the fabric bag have been claimed to be responsible for dust cake release by different investigators (*3*−*11*). Dennis et al. (*3*) demonstrated that significant cake release only occurs when the pressure pulse has an initial pressure rise rate greater than 600 Pa/ms. Rothwell (*4*, *5*) used the same criteria in the study of pulse−jet fabric filtration systems. Other authors (*6*, *7*) claimed that fabric acceleration is the main cleaning mechanism and that reverse air flow plays only a minor role.

Klingel and Löffler (*8*) pointed out that, when air pressure impulse (PI) in the fabric bag is greater than 50 Pa·s or 0.2 in. of H_2O·s, dust removal efficiency will not increase further. Air pressure impulse is defined as the integral of pressure versus time over a pulse duration or $PI = \int_0^{T_{pd}} P(t)\, dt$ (T_{pd}, pulse duration). Sievert and Löffler (*9*) further investigated the factors that influence pulse pressure signals inside the blow tube and inside the fabric bag experimentally.

Humphries and Madden (*7*) found that there is a minimum pulse pressure of about 0.3 kPa in the fabric bag which removes about 60% of the dust cake from the fabric. Increasing the pulse pressure beyond this minimum value results in only a slight increase in the amount of dust dislodgment from the bag. Löffler and Sievert (*10*) also pointed out that it is necessary to reach a critical static overpressure of 400−500 Pa at all locations along the length of a bag in order to achieve a good fabric cleaning efficiency. The overpressure is defined as the magnitude that the pressure pulse within the bag developed by the pulse−jet exceeds the operating pressure drop of the filter.

Along the direction of fabric bag, cleaning mechanisms responsible for dust release may be different. The strong acceleration/deceleration in the upper bag regions was said to be responsible for cake dislodgment, while in the lower

S0013-936X(96)00020-X CCC: $12.00

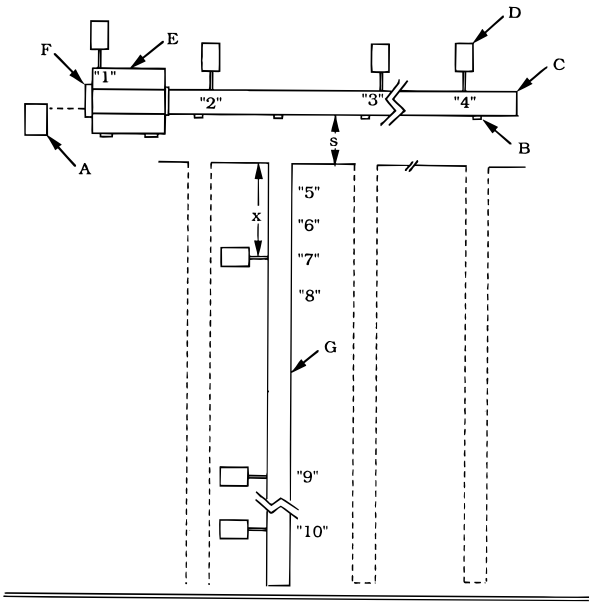

A	timer	F	diaphragm valve
B	nozzle	G	fabric bag
C	blow tube	x	distance between measured point and bag opening
D	pressure transducer	s	distance between nozzle and bag opening
E	pressure tank	"1"–"10"	position of measured point

FIGURE 1. Schematic diagram of the pulse–jet cleaning system used in this study.

bag regions the dust removal was due to the reverse air flow (*10*, *11*).

In view of the above previous experimental studies, there seems to be a need for an in-depth study of the pulse–jet cleaning process. In particular, air pressure and air flow distributions in the system, which have direct influence on the bag cleaning efficiency, have never been investigated thoroughly. In order to study the influence of various design and operational parameters on the air flow and pressure pulse distributions in the system, this research has developed an unsteady, compressible flow model for simulating the pulse–jet cleaning process. Simulated results will be compared with experimental data first. A validated numerical model is then used to study optimum design and operational parameters for a pulse–jet cleaning system.

Experimental Method

The current experimental setup is shown in Figure 1. Air flow and pressure distributions of the system will be modeled numerically based on the same system. The system consists of a blow tube (inside diameter, 8.3 cm; length, 210 cm), seven straight-bore nozzles (inner diameter, 13.5 or 26 mm; spacing between nozzles, 30 cm), 10 pressure transducers (high pressure, Dwyer Model P634-2; low pressure, Dwyer P604-2), a pulse valve (nominal diameter, 3 in.; Goyen Model CA76mms), an air pressure tank (length, 120 cm; width, 50 cm; height, 50 cm; tank volume, 0.3 m^3) and a 6-m-long bag (Ryton, inner diameter, 5.1 in.) installed under the third nozzle. The location of 10 pressure transducers in the system is as follows: point 1, air pressure tank; points 2–4, blow tubes, which are 30, 120, and 210 cm away from the air pressure tank, respectively; points 5–10, fabric bags, which are 30, 60, 90, 120, 300, and 510 cm away from the bag opening. Pulse duration ranges from 40 to 500 ms. As soon as the pulse valve is actuated, a digital data acquisition system at a sampling rate of 10 K Hz starts to take readings from the 10 transducers simultaneously until the pressure pulse is over.

The distance between the bag opening and the nozzle is adjusted from 5 to 30 cm, and the initial tank pressure is varied from 1.5–3.5 kg/cm^2. Diameter of the straight-bore nozzle is 13.5 or 26 mm. In this experiment, air tank volume, blow tube diameter, and length are fixed. To facilitate pressure pulse measurement, only a clean bag is used and there is no filtering air flow across the bag. The resistance coefficient k of the clean bag, which is defined as $k = \Delta p/v$ (v, filtration velocity; Δp, pressure drop through fabric), is measured to be 864 Pa·s m^{-1}.

Numerical Method

To model the pulse–jet cleaning system shown in Figure 1 numerically, the calculation domain is divided into four units, namely, air pressure tank, blow tube, nozzle, and fabric bag. The governing equations are described below.

Air Pressure Tank. When air is discharged from the pressure tank through the pulse valve into the blow tube, the process is very fast and can be considered as adiabatic. For isentropic flow, the tank pressure (P_{tk}) and the discharged air mass m from the pressure tank can be related as (*12*)

$$\frac{V}{\gamma}\frac{dP_{tk}}{dt} = RT_{tk}\frac{dm}{dt} \tag{1}$$

where V is the tank volume, γ is the special heat ratio or air, R is the universal gas constant, t is time, and T_{tk} is the tank temperature. If the blow tube pressure P_{bt} is less than the critical pressure, then the following equation holds (*13*):

$$\frac{dm}{dt} = -C_v A_v P_{tk}\left[\frac{\gamma}{RT_{tk}}\left(\frac{2}{\gamma+1}\right)^{\gamma+1/\gamma-1}\right]^{1/2} \tag{2}$$

If the blow tube pressure is greater than the critical pressure, then the flowing equation holds (*13*):

$$\frac{dm}{dt} = -C_v A_v P_{tk}\left[\frac{2\gamma}{\gamma-1}\frac{1}{RT_{tk}}\left(\left(\frac{P_{bt}}{P_{tk}}\right)^{2/\gamma} - \left(\frac{P_{bt}}{P_{tk}}\right)^{(\gamma+1)/\gamma}\right)\right]^{1/2} \tag{3}$$

where C_v is the valve discharge coefficient and A_v is the valve opening area.

Blow Tube. Air flowing through the pulse valve is discharged into the blow tube. If air flow is incompressible in the blow tube, then the following equation holds for the relationship between pressures at any two points in the blow tube:

$$P_{bt2} = P_{bt1} - \rho f\frac{L_{bt}}{D}\frac{v_{bt}^2}{2} \tag{4}$$

where P_{bt1} and P_{bt2} are the upstream and downstream pressure in the blow tube, L_{bt} is the distance between the two points, v_{bt} is the air velocity in the blow tube, ρ is the air density, and f is the moody friction coefficient that can be found from the Moody chart.

When the Mach number of the air flow is greater than 0.2, the flow becomes compressible. The relationship between the Mach number M and the maximum distance when flow attains sonic velocity, L_{max}, is (*14*, *15*)

$$4\bar{f}\frac{L_{max}}{D} = \frac{1-M^2}{\gamma M^2} + \frac{\gamma+1}{2\gamma}\ln\frac{(\gamma+1)M^2}{2\left(1+\frac{\gamma-1}{2}M^2\right)} \quad (5)$$

where D is the tube diameter and $\bar{f}$ is the mean friction coefficient over the pipe length L_{bt}.

Nozzle. The mass flow rate through a nozzle can be calculated based on similar equations such as eqs 2 or 3, except that nozzle discharge coefficient and area must be used, P_{tk} must be replaced by P_{bt}, and P_{bt} replaced by ambient pressure. Air flow discharged from a nozzle can be viewed as a free, turbulent circular air jet. In a free, turbulent circular jet, a number of flow regions can be distinguished (*16*). At a distance larger than about 70 nozzle diameter (d_n), the time−mean velocity profile is self-preserving in this so-called fully developed region. The first 5 d_n is called the mixing layer region while the region between 5 d_n and 70 d_n is partial self-preservation. Entrainment rate E for a free jet is defined as

$$E = \frac{d(m_z/m_0)}{d(z/d_n)} \quad (6)$$

where m_z is the mass flow rate at jet axial position z, m_0 is the mass flow rate at the jet exit $z = 0$. Depending on air flow regions and jet exit conditions (laminar or turbulent), the experimental value of the entrainment rate is between 0.15 and 0.259 (*16*). In the mixing layer region, the entrainment rate can be considered as (*16*)

$$y_{0.5} = c_{0.5}(z - z_{0,m}) \quad (7)$$

$$E = 0.9\left(\frac{dB}{dz}\right)^2\left(\frac{z - z_{0,m}}{d_n}\right) + 4c_{0.5} \quad (8)$$

where y is the radial distance of flow with the jet centerline and $y_{0.5}$ is the location where $\bar{U}_z = 0.5\bar{U}_0$. $\bar{U}_z$ is the time−mean velocity in the jet axial direction, and $\bar{U}_0$ is the velocity in the potential core. $z_{0,m}$ represents the virtual origin of the fully developed mixing layer. $C_{0.5}$ is the slope of $y_{0.5}$ line, and B is the mixing layer width.

In the region of partial self-preservation, the time−mean velocity profile in the cross section of the jet can be described as (*16*)

$$\bar{U}_z/\bar{U}_m = f(\eta) = \exp(-C\eta^2) \quad (9)$$

where $\bar{U}_m$ is the time−mean velocity on the centerline and the constant C has the value of 0.693. η is the reduced radial coordinate that is defined as

$$\eta = r/r_{0.5} \quad (10)$$

where r is the radial distance from the jet centerline and $r_{0.5}$ is the value of the location where $\bar{U}_z = 0.5\bar{U}_m$. The entrainment rate is given as

$$E = 8R^2AC_3 \quad (11)$$

where R and A are constants (*17*) and C_3 is given as

$$C_3 = \int_0^\infty \eta f(\eta)\, d\eta \quad (12)$$

In pulse−jet fabric filtration systems, the distance between nozzles and bag opening is often in the 5−70 d_n range, or the flow is often in the region of partial self-preservation. Hence eqs 9−12 are used in the calculation of the entrainment rate.

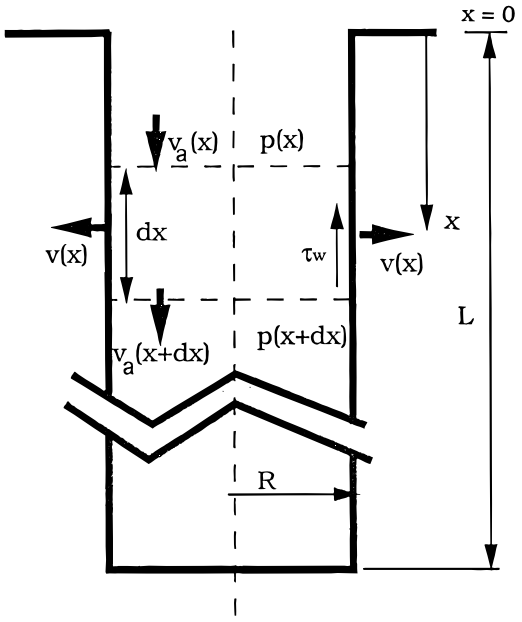

L : length of fabric bag

R : radius of fabric bag

τ_w: shear stress on bag wall

v(x) : radial volecity of air

$v_a(x)$: axial velocity of air

p(x) : air pressure

FIGURE 2. Control volume of the fabric bag.

Fabric Bag. Figure 2 shows the control volume of a fabric bag. The relationship between radial velocity $v(x)$ and axial velocity $v_a(x)$ of the air flow at a distance x from the bag opening can be found through the mass conservation principle as (*18*)

$$\rho v(x)2\pi R\, dx = -\rho\int_0^R [v_a(x + dx,r) - v_a(x,r)]2\pi r\, dr$$

or

$$v(x) = -\frac{R}{2}\frac{dv_a(x)}{dx} \quad (13)$$

where ρ is air density and r is the radial location. Applying the momentum conservation principle, the relationship between the air pressure and axial velocity of the flow can be written as

$$\rho\pi R^2\, dx\frac{\partial v_a}{\partial t} + \pi R^2\beta^2\rho[v_a^2(x + dx) - v_a^2(x)] = (P(x) - P(x + dx))\pi R^2 - \tau_w 2\pi R\, dx \quad (14)$$

where β is the Eckert's correction factor, which equals 1.1 (*19*). From Darcy's law, the relationship between air pressure and radial velocity can be written as

$$\frac{d(P(x))}{dx} = \frac{d}{dx}(k(x)v(x)) \quad (15)$$

where $k(x)$ is the resistance coefficient of the fabric bag. In

this experiment, a new bag is used and k can be considered as a constant, 864 Pa/m·sec. Shear stress at the fabric surface can be calculated as

$$\tau_w = \frac{f}{8}\rho v_a^2 \qquad (16)$$

where f is the friction coefficient of the air flow. Combining eqs 13−16, one obtains the following equation:

$$\frac{\partial v_a}{\partial t} = \frac{kR}{2\rho}\frac{\partial^2 v_a}{\partial x^2} - 2\beta^2 v_a \frac{\partial v_a}{\partial x} - \frac{f}{4R}v_a^2 \qquad (17)$$

Equation 17 can be solved by the Briley−McDonald finite difference method for $v_a(x)$ (*20*). After finding $v_a(x)$, the radial velocity $v(x)$ and pressure $p(x)$ of the air flow can be calculated.

For the present computation scheme, the input data are tank volume, initial tank pressure, blow tube diameter, nozzle diameter, bag length, bag diameter, and pressure pulse duration. At the beginning of the simulation, a small pulse valve opening area was set that corresponds to a small time step. The time step was chosen as small as 10^{-5} s. Further reduction in the time step does not increase the accuracy of computational results. For a typical pulse duration of 300 ms, there were 30 000 total computational steps that took about 15 min using an IBM 486 personal computer.

An outlet air mass flow rate of the valve was first calculated. Within each small time step, the air flows in the tank, blow tube, and nozzle are very fast and were considered to be at quasi-steady-state. The air pressure, temperature, and flow rate were then calculated at each time step for each of the first three calculation units: pressure tank, blow tube, and nozzle. The blow tube pressure was obtained when the air flow rate through the valve was equal to the sum of the flow rates through all of the seven nozzles. Then the mass flow rate through the nozzles was calculated. Finally, at each time step, air flow and pressure distributions within the fabric bag were computed by numerical integration of eq 17. The computation of the next time step continued until the desired pulse duration was over.

Results and Discussion

Comparison of Numerical Results with Experiment Data. Figure 3a−c shows the simulated results and experimental data of the tank pressure, P_{tk}, and blow tube pressure, P_{bt}, versus time under different initial tank pressures when the nozzle diameter d_n is 26 mm, the distance between the nozzle and bag opening s is 10 cm, and the pulse duration T_{pd} is 0.3 s. From these figures, it is seen that the pressure will drop with time and the computation model is capable of simulating both the pressure variation in the pressure tank and the blow tube. When the valve just opens, the blow tube pressure will rise rapidly to a level close to but still lower than that of the initial tank pressure. This is because initially the upstream and downstream pressure difference across the valve is very high. As the air is discharged from the nozzles, air pressures in both the tank and blow tube will drop with time. Depending on initial tank pressure, air pressure in the blow tube at any time is about 0.5−1.0 kg/cm^2 lower than that in the tank.

When the ratio of downstream pressure to upstream pressure of the nozzle is below the critical value (0.528),

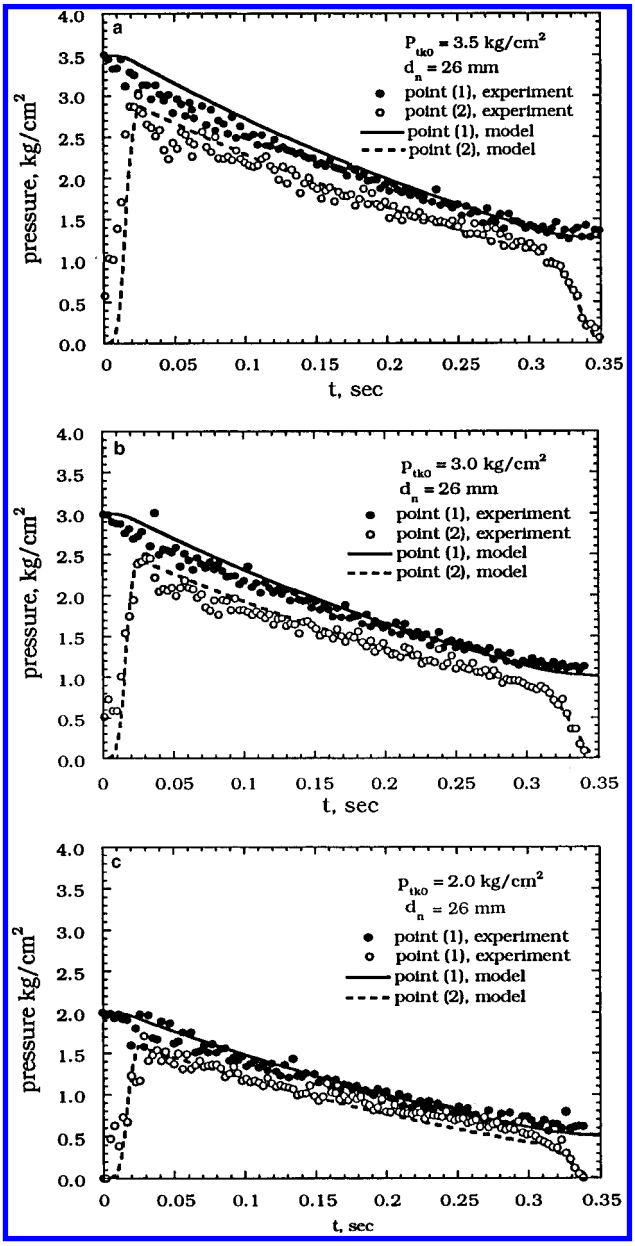

FIGURE 3. Variation of tank and blow tube air pressures with time under different initial tank air pressures.

the air mass flow rate through the nozzle is proportional to the blow tube pressure (see eq 2). This causes the pressure drop rate to be steeper when the initial tank pressure is high as seen in Figure 3a−c.

The static pressure inside the bag is one of the main parameters controlling dust cake release (*10*). Figure 4a−c shows the air pressure P_{bg} in the fabric bag versus time at points 7−10 when the initial tank pressure P_{tk0} is 3.0 kg/cm^2. The agreement between simulated results and experimental data is seen to be quite satisfactory. At point 7, after the pulse is over, there is a short period when simulated air pressure becomes negative because reverse air flow occurs. The current pressure transducer can catch only a positive pressure signal; therefore, no negative pressure data are available for comparing with simulated results.

From Figure 4a, it is seen that near the bag opening, a very high pressure peak reaching about 6 in. of H_2O in a very short time, then air pressure drops rapidly with time. Peak pressure drops rapidly with the axial distance as air

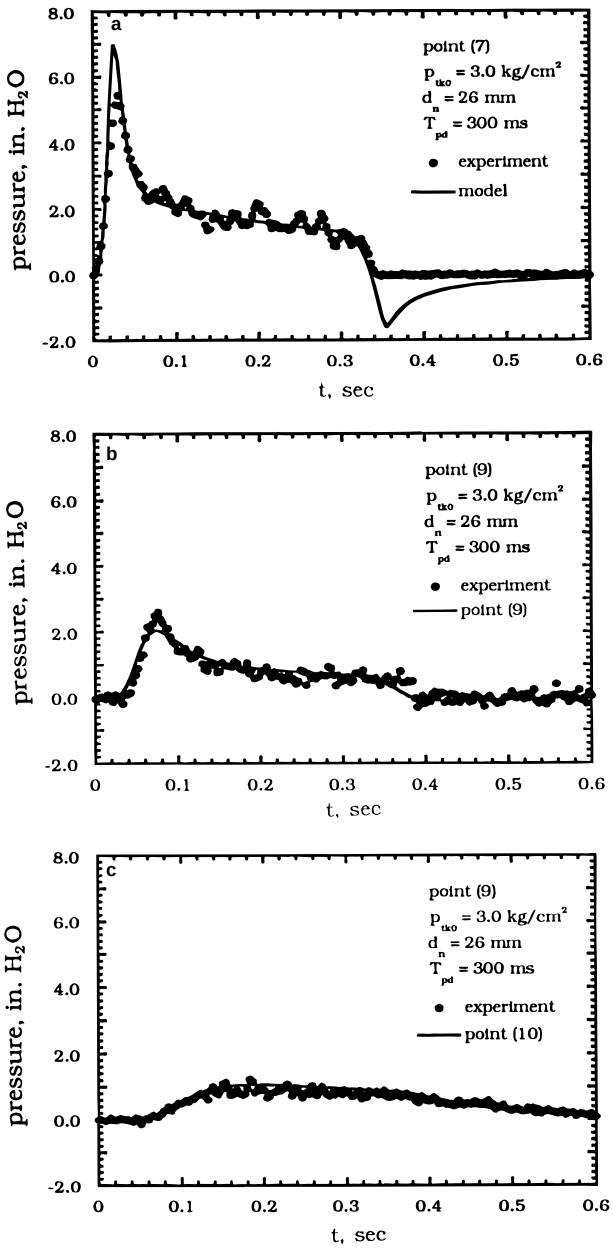

FIGURE 4. Variation of air pressure with time in the fabric bag: (a) point 7; (b) point 9; (c) point 10.

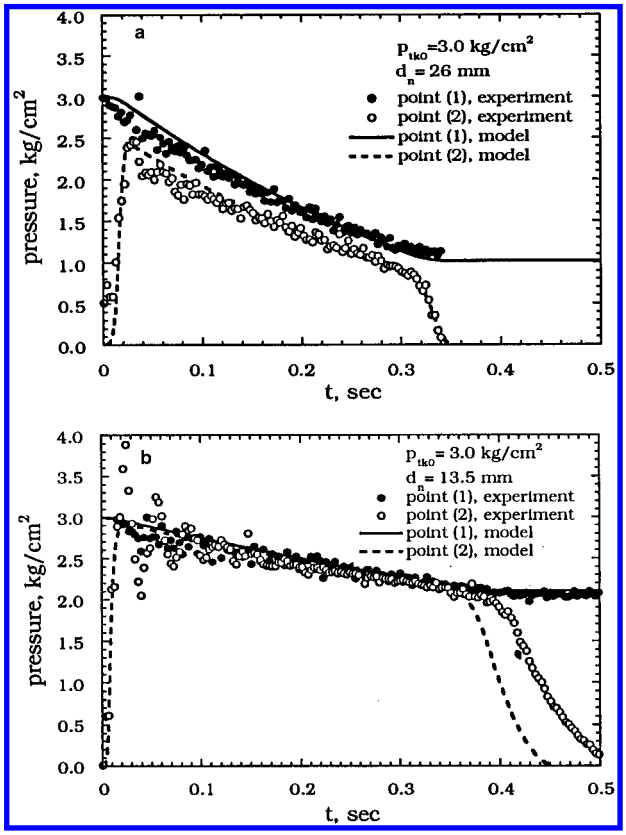

FIGURE 5. Variation of tank and blow tube air pressures with time under different nozzle diameters.

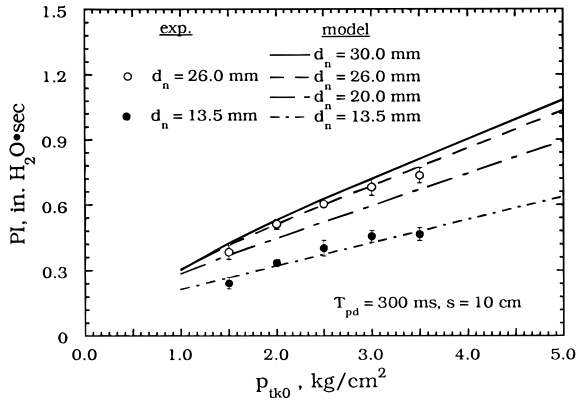

FIGURE 6. Relationship between air pressure impulse at point 7 with initial tank air pressure at different nozzle diameters.

flows radially outward while it travels downward. Peak pressure also occurs later at a lower portion of the bag as it takes time for air to travel downward. At points 9 and 10, peak pressures are only about 2 and 1 in. of H_2O, respectively (Figure 4b,c). Not only the peak pressure is high, the initial pressure rise rate is also high at the upper portion of the bag, and both drop with the axial distance along the bag.

According to the criteria set by Sievert and Löffler (*10*), the overpressure pulse in the bag must be 400−500 Pa in order to achieve good fabric cleaning efficiency. In Figure 4, the peak pressures at points 7 and 9 meet this criteria while the peak pressure at point 10 does not. In this simulation, the resistance coefficient of a new bag, 864 Pa•s m^{-1} is used. In this study, increasing resistance coefficient is found to increase the pressure pulse in the bag to an extent that the peak pressure at point 10 may exceed the criteria. The bag friction coefficient f (see eq 16) was found to be 0.22 for a best fit to the experimental data. The friction coefficient larger than that normally encountered in a pipe flow may explain that an additional energy loss occurs due to bag oscillation during the cleaning process.

Effect of Nozzle Diameter on Air Pressure Impulse. Figure 5a,b shows simulated results and experimental data of the tank and blow tube pressure versus time when the nozzle diameters are 26 and 13.5 mm, respectively. It is seen that the larger nozzle diameter makes the pressure inside tank and blow tube drop more quickly. This is because the air mass flow rate through the nozzle is proportional to the area of nozzle when other operating conditions are fixed. The simulated results agree with experimental data very well for different nozzle diameters.

Figure 6 shows the effect of nozzle diameter on pressure impulse at point 7 at different initial tank pressures, P_{tk0}. From this figure, it is seen again that the simulated results agree with experimental data very well. When the nozzle diameter increases, the pressure impulse also increases.

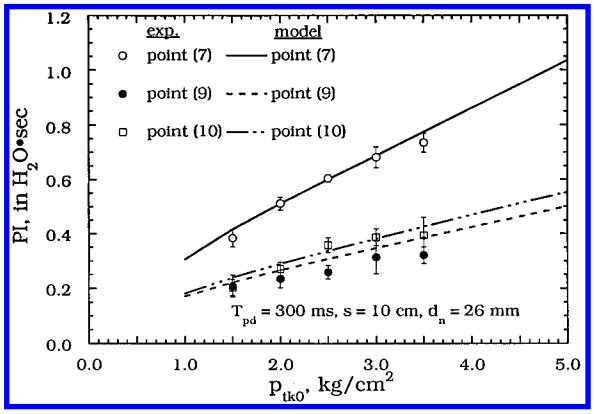

FIGURE 7. Relationship between pressure impulse with initial tank air pressure at different positions on the fabric bag.

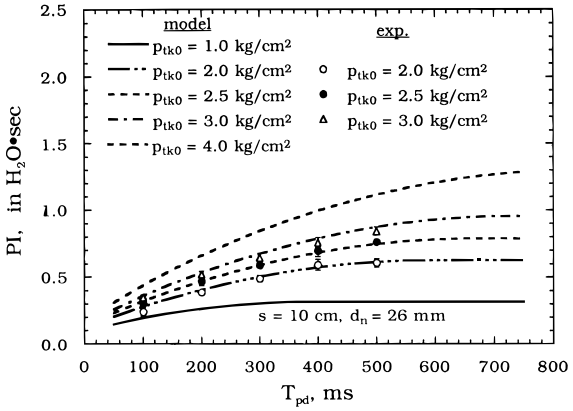

FIGURE 8. Variation of air pressure impulse at point 7 in the fabric bag with pulse duration time under different initial tank air pressures.

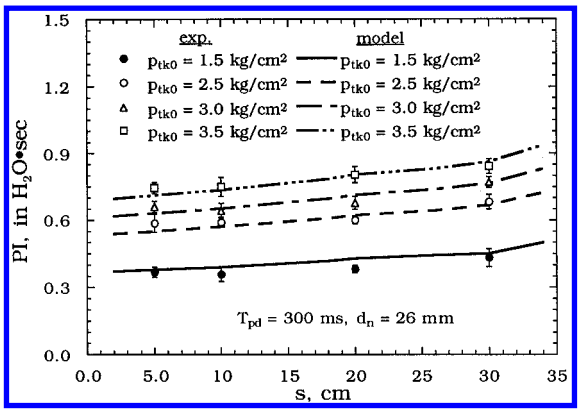

FIGURE 9. Comparison of experimental data and simulated results of pressure impulse for different distances between nozzle and bag opening under different initial tank air pressures.

But if the nozzle diameter becomes too large, the air pressure in the tank and blow tube will drop too quickly to a useless low value. This means that there is an optimum nozzle diameter for each system. Optimization of the nozzle diameter will be discussed later. For the current system when the initial tank pressure is fixed, the increase of pressure impulse for nozzle diameter ranging from 13.5 to 26 mm is seen to be significant while the gain becomes marginal when nozzle diameter increases from 26 to 30 mm.

From Figure 6, it is seen that the pressure impulse increases almost linearly with the initial tank pressure. This is because the mass flow rate from the nozzles is proportional to the tank pressure (see eqs 2 and 3).

Effect of Initial Tank Pressure on Air Pressure Impulse. Figure 7 shows the effect of initial tank pressure on pressure impulse at points 7−10. When the tank pressure increases, the bag pressure impulse is also seen to increase linearly. But the increase is more pronounced at the upper portion (point 7) and is less pronounced at the middle and lower portions of the fabric bag (points 9 and 10). That means, higher initial tank pressure always provides more cleaning force for the bag, especially at the upper portion of the bag. However, when the pressure impulse is higher than necessary, frequent damage of the bag near the top may occur.

From Figure 7, it is seen that pressure impulse at point 10 is greater than point 9. Although from Figure 4b,c, the peak pressure and average pressure pulse of point 10 are seen to be less than those at point 9, but the longer pressure pulse at point 10 more than compensates the differences to make the pressure impulse higher than that of point 9.

Effect of Pulse Duration on Pressure Impulse. Figure 8 shows the pressure impulse at point 7 under different pulse durations (T_{pd}) when initial tank pressures are 2.0, 2.5, and 3.0 kg/cm^2, respectively. From the figure, it is seen that the pressure impulse increases rapidly for pulse duration less than about 400 ms. When pulse duration is greater than 400 ms, pressure impulse levels off eventually because air pressure in the tank will then drop to a useless low value with time. Therefore, too long a pulse duration is not recommended. For example, when P_{tk0} = 2.0 kg/cm^2, the pressure impulse increases rapidly from 0.2 in. of H_2O at T_{pd} = 100 ms and reaches a constant value of 0.6 in. of H_2O·s for T_{pd} greater than 450 ms. The time to reach a steady state pressure impulse will increase somewhat at higher initial tank pressure. In the system under investigation, it is suggested that the minimum pulse duration is 300 ms, and the maximum duration time is 450, 500, and 600 ms for P_{tk0} = 2.0, 2.5, and 3.0 kg/cm^2, respectively.

Effect of Distance between Nozzle and Bag Opening on Pressure Impulse. Figure 9 shows the effect of different distances between nozzle and bag opening on pressure impulse at point 7. The distances are 5, 10, 20, and 30 cm, respectively. Both experimental data and simulated results show that when the distance increases, the pressure impulse also increases. The increase in pressure impulse for ranging from 5 to 30 cm is about 10% for different initial tank pressures investigated. The experimental data of Rothwell (*4*) also show similar trend. Increase of the pressure impulse with the distance is because a longer distance between the nozzle and bag opening will allow more induced secondary air flow into the bag, which will result in an increase of pressure impulse in the bag. However, if the distance becomes too long, the spreading width of the nozzle exit flow at the bag opening may become greater than the bag diameter. Eventually only part of the nozzle and induced air flow will be pulsed into the bag, which may result in lower pressure impulse. That is, there is an optimum distance depending on nozzle and bag diameters. Optimization of this distance will be discussed in the next section.

Optimization of Design and Operational Parameters. From the discussion above, it is found that the most important parameters influencing static pressure and pressure impulse inside the bag are nozzle diameter, distance between nozzle and bag opening, pulse duration, initial tank pressure, and tank volume.

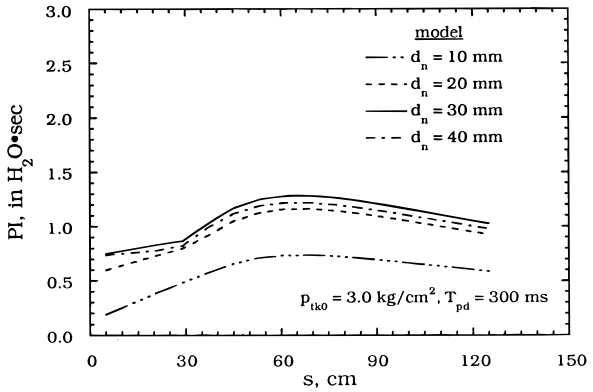

FIGURE 10. Relationship between air pressure impulse and distance between nozzle and bag opening when P_{tk0} = 3.0 kg/cm^2.

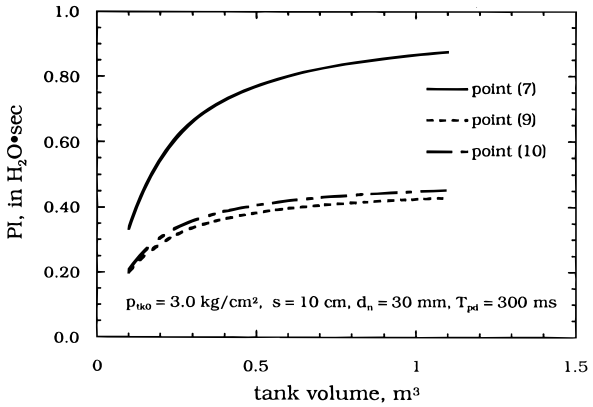

FIGURE 11. Relationship between pressure impulse at different locations of the bag and tank volume, when nozzle diameter is 30 mm, P_{tk0} = 3.0 kg/cm^2, and distance between nozzle and bag opening is 10 cm.

In Figure 10, the effect of the distance between nozzle and bag opening on pressure impulse at point 7 under different nozzle diameters has been studied for the current system. The maximum PI of 0.75 in. of H_2O•s occurs at the nozzle diameter of 30 mm for P_{tk0} = 3.0 kg/cm^2. Nozzle diameter greater than 30 mm will result in a decrease in pressure impulse. For P_{tk0} other than 3.0 kg/cm^2, the optimum nozzle diameter is also found to be 30 mm in other separate runs. For any other pulse−jet cleaning system, an optimum nozzle diameter may be different and can be calculated for a maximum PI using the current numerical method.

Figure 10 also shows the effect of the distance between the nozzle and the bag opening on pressure impulse at point 7. The figure shows that there is a maximum PI occurring at a certain distance corresponding to a fixed initial tank pressure. It is seen that when the nozzle diameter is 30 mm and the distance between nozzle and bag opening is 60 cm, the maximum PI can often be obtained. In general, the pressure impulse increases when the nozzle diameter increase from 10 to 30 mm. However, when the nozzle diameter becomes 40 mm, it is seen that the pressure impulse becomes less than the case of 30 mm since only part of the nozzle and induced flow will enter the fabric bag.

The pressure tank volume of 0.3 m^3 has been used in previous sections. The effect of increasing pressure tank volume on pressure impulse is investigated further. Figure 11 shows the relationship of pressure impulse at different locations of the bag with the tank volume, when the nozzle diameter is 30 mm, P_{tk0} = 3.0 kg/cm^2 and the distance between the nozzle and bag opening is 10 cm. It is seen that pressure impulse on the bag levels off when the tank volume is greater than about 0.5 m^3. This is because the pressure does not decrease too much further with time in the blow tube when the tank volume is greater 0.5 m^3. For the current system, it is suggested that the tank volume between 0.3 and 0.5 m^3 is acceptable.

Acknowledgments

The authors acknowledge the financial support by the Taiwan National Science Council under Contract NSC 83-0618-E-009-057.

Literature Cited

(1) Bustard, C. J.; Cushing, K. M.; Chang, R. L. *J. Air Waste Manage. Assoc.* **1992**, *42*, 1240.
(2) Dennis, R.; Wilder, J. E.; Harmon, D. L. *J. Air Pollut. Control Assoc.* **1981**, *31*, 987.
(3) Lanois, G. D.; Wiktorsson, A. *Current Status and Future Potential for High-Ratio Fabric Filter Technology Applied to Utility Coal-Fired Boilers*; EPRI report; EPRI: Palo Alto, CA, 1982.
(4) Rothwell, E. *Filtr. Sep.* **1988**, *25*, 257.
(5) Rothwell, E. *Filtr. Sep.* **1990**, *27*, 345.
(6) Ellenbecker, M. J.; Leith, D. *Filtr. Sep.* **1981**, *18*, 41.
(7) Humphris, W.; Madden, J. J. *Filtr. Sep.* **1983**, *20*, 40.
(8) Klingel, R.; Löffler, F. *Proceedings of the Filtech Conference*; London, 1983; p 306.
(9) Sievert, J.; Löffler, F. *Proc. Conf. Particulate Multiphase Process* **1985**, *II*, 647.
(10) Sievert, J.; Löffler, F. *Chem. Eng. Process* **1989**, *26*, 179.
(11) Löffler, F.; Sievert, J. *Filtr. Sep.* **1987**, 110.
(12) Sadd, M. A. *Compressible Fluid Flow*; Prentice-Hall, Inc.: Englewood Cliffs, NJ, 1985; p 98.
(13) Kayser, J. C.; Shambaugh, R. L. *Chem. Eng. Sci.* **1991**, *46*, 1697.
(14) Fox, R. W.; McDonald, A. T. *Introduction to Fluid Mechanics*, 3rd ed.; John Wiley & Sons: New York, 1973; p 631.
(15) Shapiro, A. H. *The Dynamics and Thermodynamics of Compressible Fluid Flow;* John Wiley & Sons: New York, 1953; p 167.
(16) Fondse, H.; Leijdens, H.; Ooms, G. *Appl. Sci. Research* **1987**, *40*, 355.
(17) Hinze, J. O. *Turbulence*, 2nd ed.; McGraw-Hill Book Co.: New York, 1975; p 538.
(18) Schmidt, E.; Löffler, F. *EPRI Ninth Particular Control Symposium*, Willamsburg, October 15−18, 1991; EPRI: Palo Alto, CA, 1991.
(19) Olson, R. M.; Eckert, E. R. G. *J. Appl. Mech.* **1966**, *Mar*, 7.
(20) Anderson, D. A.; Tannehill, J. C.; Pletcher R. C. *Computational Fluid Mechanics and heat Transfer*; McGraw-Hill Book Co.: New York, 1984; p 65.

Received for review January 11, 1996. Revised manuscript received June 13, 1996. Accepted June 20, 1996.[⊗]

ES960020U

[⊗] Abstract published in *Advance ACS Abstracts*, September 15, 1996.